

Experimental Investigation of Initial Steps of Helix Propagation in Model Peptides[†]

Grażyna Goch,[‡] Maciej Maciejczyk,[‡] Marta Oleszczuk,[‡] Damian Stachowiak,[§] Joanna Malicka,^{||} and Andrzej Bierzyński^{*‡}

Institute of Biochemistry and Biophysics, Polish Academy of Sciences, ul. Pawińskiego 5A, 02-106 Warsaw, Poland, Institute of Biochemistry and Molecular Biology, University of Wrocław, Tamka 2, 50-137 Wrocław, Poland, and Faculty of Chemistry, University of Gdańsk, J. Sobieskiego 18, 80-952 Gdańsk, Poland

Received December 10, 2002

ABSTRACT: It is not certain whether the helix propagation parameters s_n (i.e., the equilibrium constants between $(n - 1)$ - and n -residue long α -helices) determined from numerous studies of rather long model peptides are applicable for description of the initial steps of the helix formation during the protein folding process. From fluorescence, NMR, and calorimetric studies of a series of model peptides, containing the La^{3+} -binding sequence nucleating the helix (Siedlecka, M., Goch, G., Ejchart, A., Sticht, H., and Bierzyński, A. (1999) *Proc. Natl. Acad. Sci. U.S.A.* 96, 903–908), we have determined, at 25 °C, the average values of the enthalpy ΔH_n and of the helix growth parameters s_n describing the first four steps of helix propagation in polyalanine. The absolute values of the C-cap parameters, describing the contribution of the C-terminal residues to the helix free energy, have also been estimated for alanine (1.2 ± 0.5) and NH_2 group (1.6 ± 0.7). The initial four steps of the helix growth in polyalanine can be described by a common propagation parameter $s = 1.54 \pm 0.04$. The enthalpy ΔH_n is also constant and equals $-980 \pm 100 \text{ cal mol}^{-1}$.

Intensive experimental studies of the helix–coil transition in polypeptide chains have been carried out in the last three decades, with the aim to elucidate factors determining the stability of the α -helical conformation (1–3). The strategy of the experiments as well as the basis of data analysis have been provided by the theory formulated in early 1950s by Zimm and Bragg (4), and using a somewhat different formalism, by Lifson and Roig (5). According to this theory, two fundamental parameters describe α -helix stability, called the initiation and propagation factors (σ and s , respectively, using the Zimm–Bragg notation), and the statistical weight of an α -helical segment containing j hydrogen bonds between i and $i + 4$ residues is given by

$$k_j = \sigma s^j \quad (1)$$

The theory was formulated for homopolymers and in the case of native peptides had to be modified by introduction of different s values for different amino acid residues. It also turned out that numerous corrections for specific side chain–side chain and charge–helix dipole interactions, as well as N- and C-cap effects had to be included (6). In particular, it was found that the statistical weight of the last residues at both N- and C-termini of helix segments that participate in a helix hydrogen bond network but whose φ and ψ backbone angles are not restricted should be described by N- and C-cap parameters, n and c , respectively, different from s .

In its modified form the theory provides, in practice, quite a good tool (7), and in fact, the only one with which to describe the helix–coil transition, although the strict correctness of its fundamental assumptions is still debated (8).

One of the objections raised against the theory, even when applied to homopolymers, is that it assumes that propagation parameters do not depend on helix length (i.e., that the Gibbs free energy of including the first (ΔG_1), second (ΔG_2), and so on residues into the helical conformation is the same as ΔG_∞ , describing elongation of a very long α -helix by one residue). There is no reason to believe that this assumption is correct. In fact, one can readily produce arguments that it is not.

Because the conformation of short helices is more flexible, the initial propagation steps should cause a smaller entropy drop than the propagation of long helices since the net effect of the latter process is an elongation of the central, rigid part of a helix. Moreover, in short helices the backbone groups are more accessible to water because a large fraction of them does not form internal hydrogen bonds. Therefore, because of solvation effects, the enthalpy of the first propagation steps should be much more favorable (9).

On the other hand, two opposite effects must be taken into account: first, the absence, in short helices, of long-range dipole–dipole interactions between peptide groups that stabilize considerably the α -helical conformation (10, 11); second, because the entropy cost of 3_{10} helix formation is smaller, this conformation is often found at helix termini and can be expected to predominate in very short helices when the helix ends practically meet with each other (12–14). Consequently, the initial helix propagation parameters, determined experimentally, describe rather the coil to 3_{10} ($s_{3/10}$) than the coil to α -helix (s_α) transition. Now, the values

[†] This work was supported by Polish Committee for Scientific Research Grant 6 P04 009 16.

^{*} To whom correspondence should be addressed. Telephone: (48 22) 659-70-72 ext. 2371. Fax: (48 22) 823-71-94. E-mail: ajb@ibb.waw.pl.

[‡] Polish Academy of Science.

[§] University of Wrocław.

^{||} University of Gdańsk.

AcLoopNH ₂	Ac D K D G D G Y I S-A-A-E NH ₂
or, alternatively,	$\overline{x} \quad \overline{y} \quad \overline{z} \quad -\overline{y} \quad -\overline{x} \quad -\overline{z}$
AcLoopA ₀ NH ₂	metal binding loop
AcLoopA ₁ NH ₂	Ac D K D G D G Y I S-A-A-E A NH ₂
AcLoopA ₂ NH ₂	Ac D K D G D G Y I S-A-A-E A A NH ₂
AcLoopA ₃ NH ₂	Ac D K D G D G Y I S-A-A-E A A A NH ₂
AcLoopA ₄ NH ₂	Ac D K D G D G Y I S-A-A-E A A A A NH ₂
AcLoopGAGANH ₂	Ac D K D G D G Y I S-A-A-E G A G A NH ₂

FIGURE 1: Peptide sequences. The positions, in the Cartesian framework, of ligands coordinating La³⁺ ion are indicated. The bars indicate the three peptide groups fixed in a helical conformation by metal binding.

of $s_{3/10}$ parameters were evaluated to be at least two times smaller than those of s_{α} (12).

Therefore, the s values determined from the studies of long helices composed of more than 10 amino acid residues are, maybe, quite different—smaller or larger—than the initial helix propagation parameters and cannot be used to describe the helix formation during the protein folding process or the stability of helices built of less than 10 residues, predominating in protein structures (15).

The aim of this work was to find out how the propagation parameters depend on the helix length and to determine the Gibbs free energies (ΔG_i) and enthalpies (ΔH_i) of consecutive helix propagation steps in polyalanine. Although this problem has been addressed in a number of theoretical studies, still it remains a challenge for experimentalists because short helices are marginally populated because of (see eq 1) the low value of nucleation parameter σ , even for 3₁₀ helices (12).

Various strategies have been proposed to promote the helix initiation in polypeptides, viz. to increase the σ value, including artificial templates and covalent or metal-induced side chain—side chain cross-links (16–23). All of them are far from the ideal system that should provide a 100% populated nucleation site with conformation close to that of a helix nucleus formed spontaneously during the coil to helix transition in natural polypeptides. A system recently proposed by us (24), derived from calcium-binding loops of EF-hand proteins, does meet these requirements.

A 12-residue long synthetic peptide, analogous to the IIIId calcium-binding loop of calmodulin (see Figure 1), has a strong affinity for lanthanide ions, and in the met form it assumes a well-defined structure with the φ and ψ angles of the last three residues—Ala 10, Ala 11, and Glu 12—confined to the helical region of the Ramachandran plot with one regular α -helix hydrogen bond between the Ser 9 carbonyl and the NH₂ C-terminal group. This provides a nucleus for formation of a helix by residues attached to its C-terminus.

Comparative studies of a series of peptides, composed of the metal-binding loop (AcLoop-) with the sequence Ac-DKDGDGYISAAE- and of the C-terminal segment -A_nNH₂, where $n = 0/4$ (Figure 1), presented in this paper, provide insight into the thermodynamics of the very first steps of the propagation of the helical conformation in polyalanine. In these peptides, the N- and C-termini of the α -helix, built of residues not hydrogen-bonded by their amide and carbonyl groups, respectively, merge with each other. Only in the longest helix of Ac-DKDGDGYISAAEA₄NH₂ peptide the

Table 1: Equilibrium Constants and Gibbs Free Energies of La³⁺ Ion Binding to AcLoopA_nNH₂ Peptides

n	K_n (10 ⁵ M ⁻¹)	ΔG_m (cal mol ⁻¹)	$\Delta\Delta G_m$ (cal mol ⁻¹)	$\Delta\Delta G_m^a$ (cal mol ⁻¹)
0	1.4 ± 0.2	-7070		
1	2.5 ± 0.9	-7420	-350	-390
2	4.3 ± 0.9	-7740	-670	-740
3	5.8 ± 0.8	-7920	-850	-960
4	7.5 ± 0.9	-8070	-1000	-1150

^a Corrected for residual helix content in the metal-free peptides (see text).

central Ala13 residue forms the regular $i \rightarrow i + 4$ and $i \rightarrow i - 4$ hydrogen bonds with NH₂ group and carbonyl of Ser 9, respectively.

MATERIALS AND METHODS

Peptide Synthesis, Purification, and Sample Preparation. The peptide Ac-DKDGDGYISAAEGAGANH₂ was ordered in GenScript Corporation. The other peptides were synthesized using Fmoc chemistry and cleaved using standard procedures. All peptides were purified by reverse-phase HPLC chromatography on Vydac C18 column. After each experiment, the peptide sample was checked by analytical HPLC¹ chromatography, and if the level of detected impurities exceeded 3% the measurement results were rejected.

Peptide samples were prepared in 20 mM Pipes buffer for fluorescence measurements, 20 mM cacodylic buffer for calorimetric measurements, and 2 or 20 mM Tris buffer for CD and NMR experiments, respectively, 0.1 M NaCl, pH 6.9, by dilution of concentrated stock solutions. Peptide concentration in the stock solutions, prepared freshly before experiments, was determined from tyrosine UV absorbance measured at 280 and 274 nm using the extinction coefficients equal 1197 and 1394 M⁻¹ cm⁻¹, respectively (25).

CD Measurements. The CD spectra were recorded on an Aviv Model 202 spectropolarimeter equipped with a HP Model 89100A temperature controller. All measurements were carried out at 25 °C in a 10 mm path-length cell with a peptide concentration of ca. 10 μ M.

Fluorescence Measurements. Tyrosine luminescence signal of the peptides excited at 280 nm was measured using an apparatus described previously (26). Ln³⁺ ion coordination constants of the peptides were determined from titration measurements of Tyr7 fluorescence intensity and least-squares fit of theoretical curves to experimental data using the NiceFit program.

Each experiment was repeated independently several times, starting from preparation of fresh samples: two times for AcLoopA₂NH₂ and AcLoopA₃NH₂ peptides; three times for AcLoopA₁NH₂, AcLoopA₄NH₂, and AcLoopGAGANH₂ peptides; and four times for the AcLoopNH₂ peptide. Error estimations shown in Table 1 have been made from mean square deviations of the results using the Student's distribution with the reliability factor of 80%.

NMR Measurements. NMR spectra of 2 mM peptide samples were recorded at 25 °C on a 500 MHz Varian spectrometer. The exchange rates of amide protons were

¹ Abbreviations: CD, circular dichroism; HPLC, high-performance liquid chromatography; NMR, nuclear magnetic resonance; rmsd, root-mean-square deviation; TFE, trifluoroethanol; UV, ultraviolet.

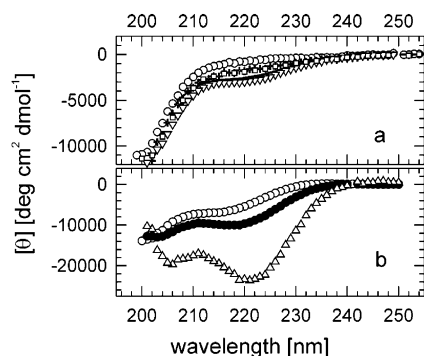


FIGURE 2: CD spectra of (a) metal-free peptides: \circ , AcLoopNH₂; $+$, AcLoopA₁NH₂; \square , AcLoopA₂NH₂; $-$, AcLoopA₃NH₂; and ∇ , AcLoopA₄NH₂. (b) La³⁺ saturated peptides: AcLoopNH₂, (\circ); AcLoopA₄NH₂, (\bullet); and their difference spectrum, (Δ); defined as $[17 \times \theta(\text{AcLoopA}_4\text{NH}_2) - 13 \times \theta(\text{AcLoopNH}_2)]/4$.

measured using the magnetization transfer method (case II) (27). Water signal was suppressed prior to acquisition using the WATERGATE sequence (28). The relaxation rate of water protons was determined in an independent experiment using inversion recovery technique (29) avoiding radiation dumping effects. Each measurement was repeated two times. The mean square deviations of the results were estimated at 10%.

Titration Calorimetry. Calorimetric titrations were carried out using a CSC 4200 isothermal titration calorimeter (Calorimetry Sciences Corp., American Fork, Utah) and software supplied with the instrument. The experiments were done according to the method described by Wiseman et al. (30). The titration was performed by 15 small injections of LaCl₃ solution. The peptide concentration ranged from 10 to 40 μM , while the concentration of the titrant ranged from 1 to 5 mM. The data were analyzed using ITCDataWorks and BindWorks programs (both supplied by the manufacturer) and were fitted according to an independent set of binding sites model to get m , K_n , and ΔH_m values. Each ΔH_m value given in Table 4 is an average from at least three up to six independent experiments. The error, estimated from mean square deviation of the results, equals $\pm 50 \text{ cal mol}^{-1}$. The number of binding sites (m) was always close to unity $\pm 1\%$, and the best-fit binding constants, not referred to in this paper, lay within the region of $1.5 \times 3 \times 10^5 \text{ M}^{-1}$. The simulations have shown that if they are fixed to the values obtained from much more precise fluorescence measurements, the calculated binding heats remain, in practice, the same.

Calculation of c_A , c_N , and s_n Parameters. The Nelder–Mead simplex method (31) was used to minimize the rmsd- (c_A, c_N) function. Calculations were carried out with program package MATLAB at the Interdisciplinary Center for Mathematical and Computational Modeling, Warsaw, Poland.

RESULTS

CD Measurements. The CD spectrum of metal-free AcLoopNH₂ peptide is very close to that characteristic of the coil conformation (Figure 2a). A small inflection around 220 nm observed in the spectra of AcLoopA_nNH₂ peptides indicates that some other, nonrandom, conformation becomes slightly populated with an increasing number of alanine

residues (n). The shapes of the spectra suggest that it is the helical conformation, as can be expected in alanine-rich peptides.

Therefore, all further data analysis has been done in two steps. In the first, we have assumed that the population of the helix in the apo peptides is negligible and that their conformation is random. In the second step, corrections because of the inadequacy of this assumption have been introduced.

The CD spectra of the peptides change dramatically in the presence of La³⁺ ions (Figure 2b). The difference spectrum of metal-saturated AcLoopA₄NH₂ and AcLoopNH₂ peptides is characteristic of the helical conformation with minima at 205 and 222 nm. The 222 band is significantly more intense than the 205 one, as predicted (32) and observed (33) in short helices composed of few peptide groups. Analogous difference spectra obtained for the other AcLoopA_nNH₂ peptides are, within error, the same (not shown). Therefore, it is evident that upon metal binding the -A_nNH₂ segments assume predominantly a helical conformation and that the helix population is closely similar in all of them.

The CD signal at 222 nm of all met-AcLoopA_nNH₂ peptides remains constant, independently of TFE concentration up to 65% (not shown). Hence, as in the case of AcLoopA₃QNH₂ peptide studied previously (24), we can conclude that the helix population in -A_nNH₂ segments equals at least 70% in the La³⁺-saturated peptides.

Fluorescence Measurements. Relative fluorescence quantum yields of Tyr 7 (data not shown) are, within error, the same for all metal-free peptides, suggesting that their local conformation in the vicinity of this residue is very similar, in line with the assumption of their predominantly random conformation. Upon binding of La³⁺ ion the tyrosine fluorescence signal drops by 49%, except in the case of AcLoopA₄NH₂ peptide, which shows a somewhat smaller fluorescence decrease, viz. 45%.

Fluorescence intensity measurements provide, therefore, a convenient and precise tool for determination of the metal-to-peptide coordination constants, K_n . Values of K_n determined from the fluorescence titration curves are given in Table 1. The binding constant to AcLoopNH₂ (K_0) is quite high ($1.4 \times 10^5 \text{ M}^{-1}$), and it increases systematically with the length of the -A_nNH₂ segment.

Thermodynamic Model of Metal Coordination. The observed dependence of K_n on n can be rationalized in the following way. The total Gibbs free energy of the lanthanum binding to AcLoopA_nNH₂ peptide

$$\Delta G_m = -RT \ln K_n \quad (2)$$

is the sum of contributions arising from (1) conformational rearrangement of the AcLoop-segment necessary for metal coordination, ΔG_{Ln} , (2) coordination of La³⁺ ion to the loop, ΔG_c , and (3) conformational transition within -A_nNH₂ segment induced by the metal coordination, ΔG_{An} . Therefore,

$$\Delta G_m = \Delta G_c + \Delta G_{Ln} + \Delta G_{An} \quad (3)$$

ΔG_c is the same for all peptides, in other words independent of n . ΔG_{Ln} is also constant if in the absence of metal ions the free energy of interactions between AcLoop- and -A_nNH₂ segments is negligible. Our basic assumption that the conformation of metal-free peptides is random implies that

this condition is fulfilled. In contrast, ΔG_{An} , arising from conformational transition of the $-A_n\text{NH}_2$ peptide segments from a random to a partially helical state, strongly depends on n . Therefore,

$$\Delta\Delta G_m = -RT \ln(K_n/K_0) = \Delta G_{An} - \Delta G_{A0} \quad (4)$$

If, as follows from eq 4, the observed increase of La^{3+} binding constant with the peptide length is due uniquely to the free energy of the coil-to-helix transition in the peptide C-terminal segment, segments that are not able to form the helix should have no effect on the loop binding affinity. $-\text{GAGANH}_2$ segment of the peptide AcLoopGAGANH_2 remains in coil conformation even after the lanthanide ion coordination because of strong helix-braking properties of the glycine residue. And indeed, as expected, the binding constant of La^{3+} to AcLoopGAGANH_2 peptide ($1.3 \pm 0.2 \cdot 10^5 \text{ M}^{-1}$) is, within error, the same as that to the loop alone ($1.4 \pm 0.2 \cdot 10^5 \text{ M}^{-1}$; see Table 1).

In the case of the AcLoopNH_2 peptide, the coil-to-helix transition at its C-terminus is reduced to partial formation of a hydrogen bond between one of the terminal NH_2 protons and backbone carbonyl groups of Ser 9 and Ala 10, characteristic of the α - or 3_{10} -helix, respectively, resulting in free energy change ΔG_{A0} . The partition function describing the conformation of NH_2 group $Z_0 = 1 + c_N$, where c_N is the equilibrium constant of hydrogen bonding, which is identical with the C-cap parameter of the amide group. Therefore,

$$\Delta G_{A0} = -RT \ln Z_0 = -RT \ln(1 + c_N) \quad (5)$$

In $-A_n\text{NH}_2$ segments of $\text{AcLoopA}_n\text{NH}_2$ peptides, the helix propagates step by step from the nucleus formed by the peptide groups between Ser 9, Ala 10, Ala 11, and Glu 12 by incorporation of consecutive peptide groups i located between Glu 12 and Ala 13 ($i = 1$), Ala 13 and Ala 14 ($i = 2$), and so on, finally including the C-terminal peptide group between A(12 + n) residue and the NH_2 C-cap group. Assuming that c_N and C-cap parameter of alanine, c_A , are constant, independently of helix length, the statistical weight of $-A_n\text{NH}_2$ segments with only one hydrogen bond, formed by the amide proton of Ala 13, equals

$$k_1 = c_A \quad (6)$$

whereas that of longer helical species containing number j of hydrogen bonds ranging from 2 up to n :

$$k_{n,j} = c_A \prod_{i=1}^{j-1} s_{n,i} \quad (7)$$

and finally, the statistical weight of the full helices, including the C-terminal peptide group, equals

$$k_{n,n+1} = c_N \prod_{i=1}^n s_{n,i} \quad (8)$$

The aim of this work is to find out whether and how the helix propagation parameters $s_{n,i}$ depend on i . Unfortunately, it cannot be assumed that they are independent of n . For example, the parameters of the first steps of the helix propagation in $\text{AcLoopA}_1\text{NH}_2$ and $\text{AcLoopA}_4\text{NH}_2$ peptides

($S_{1,1}$ and $S_{4,1}$, respectively) can be different because the presence of unordered alanine residues at the C-terminus may affect the propensity of Ala 13 for helical conformation (e.g., because of solvation effects (9)). Therefore, for each n we replace the set of $s_{n,i}$ values by an average parameter s_n , so that by definition

$$k_{n,j} = c_A s_n^{(j-1)} \quad (9)$$

and

$$k_{n,n+1} = c_N s_n^n \quad (10)$$

Consequently, the partition functions for the helix-coil transition in metal-saturated $\text{AcLoopA}_n\text{NH}_2$ peptides equal

$$Z_1 = 1 + c_A + c_N s_1 \quad (11)$$

for $n = 1$ and for $n \geq 2$

$$Z_n = 1 + \sum_{j=1}^{n+1} k_{n,j} = 1 + c_A \sum_{j=0}^{n-1} s_n^j + c_N s_n^n \quad (12)$$

Therefore, since $\Delta G_{An} = -RT \ln Z_n$, according to eq 4,

$$\Delta\Delta G_m = -RT \ln(Z_n/Z_0) = -RT \ln(K_n/K_0) \quad (13)$$

Determination of the Helix Propagation Parameters s_n . The ratios of La^{3+} binding constants K_n/K_0 determined from fluorescence measurements, shown in Table 1, are not sufficient to solve the set of four equations defined by eq 13 containing, besides four s_n , two additional unknown parameters c_A and c_N (see eqs 11 and 12). This problem has been solved in the following way.

In principle, the population of hydrogen bond(s) formed by an amide proton can be determined from measurements of its exchange rate with water. The protection parameter p , defined as the ratio of the measured exchange rate constant k_{ex} and the reference one k'_{ex} , expected in the absence of hydrogen bonding, is related in a simple manner with the fractional population, x , of hydrogen bond(s) the amide proton is involved in

$$p = k'_{\text{ex}}/k_{\text{ex}} = 1/(1 - x) \quad (14)$$

Results of our NMR measurements of the exchange protection factors for amide protons in met- $\text{AcLoopA}_n\text{NH}_2$ peptides (unpublished data) show a high content of helical conformation in $-A_n\text{NH}_2$ segments and are consistent with a step-by-step process of the helix elongation. Unfortunately, they are not precise enough to calculate the populations of various partially helical states, mainly because of errors in evaluation of the reference k'_{ex} values.

The NH_2 protons of the C-cap group are, in this respect, exceptional. Chemically they are equivalent. In all apo- $\text{AcLoopA}_n\text{NH}_2$ peptides their exchange rates, measured by the NMR magnetization transfer method, are (within error) the same, although their signals are sharp and well-separated from each other. It can be expected, then, that the ratio of their exchange rates determined from a single NMR experiment (i.e., the relative protection factor p_{NH} of one of them) can be used as a measure of the population x_{NH} of the full helix, including the C-terminal Ala- NH_2 peptide group. On

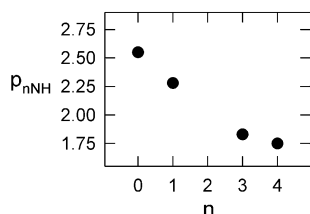


FIGURE 3: Ratio of proton exchange rates of the C-terminal amino group in met- AcLoopA_nNH₂ peptides determined from NMR magnetization transfer experiments. The exchange rates for NH₂ protons in AcLoopA₂NH₂ could not be measured because of overlap of their NMR signals with other proton signals of the peptide.

Table 2: Populations of Full Helices (x_{nNh}), Average Helix Propagation Parameters (s_n), and Fractional Population of Hydrogen Bonds (x_{nh}) in -A_nNH₂ Segments of La³⁺ Saturated AcLoopA_nNH₂ Peptides

n	$x_{nNh}^{\text{exp } a}$	$x_{nNh}^{\text{cal } b}$	s_n	s_n^{*c}	x_{nh}
0	0.61 ± 0.04	0.61			0.61
1	0.56 ± 0.04	0.56	1.63 ± 0.56	1.73 ± 0.60	0.67
2	nd ^d	0.53	1.63 ± 0.19	1.76 ± 0.21	0.73
3	0.45 ± 0.05	0.46	1.46 ± 0.07	1.59 ± 0.08	0.73
4	0.43 ± 0.05	0.42	1.38 ± 0.05	1.50 ± 0.05	0.74

^a Determined from NMR experiments. Errors correspond to 10% mean square deviations of p parameters (see eq 14). ^b Calculated from eq 15 for $c_A = 1.0$, $c_N = 1.56$, and s_n values listed in the next column. ^c Corrected for residual helix content in the metal-free peptides; $c_A = 1.2$ and $c_N = 1.56$ (see text). ^d nd: not determined because of NMR signal overlap.

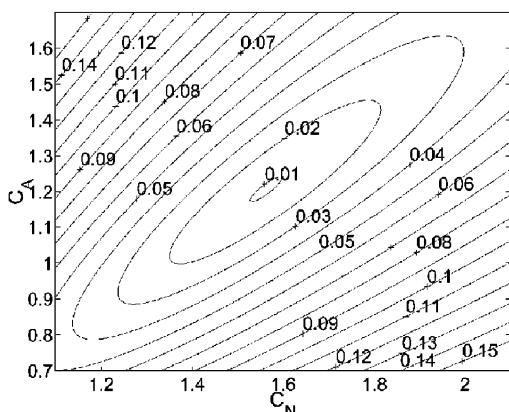


FIGURE 4: Map of rmsd(c_A, c_N) function between determined from NMR experiments $x_{nNh}^{\text{exp}(1)}$ and calculated $x_{nNh}^{\text{cal}(2)}$ populations of full helices in met-AcLoopA_nNH₂ peptides.

the other hand, this population can be calculated from the equation

$$x_{nNh}^{\text{cal}} = c_N s_n^n / Z_n \quad (15)$$

The measured relative protection factors p_{nNH} are shown in Figure 3, and x_{nNh}^{exp} values determined from them according to eq 14 are listed in Table 2.

The s_n parameters were calculated from eqs 11–13 with K_n values listed in Table 1 and variable c_N and c_A parameters. The best agreement between x_{nNh}^{exp} and x_{nNh}^{cal} (in terms of minimum rmsd of 0.01) is found for $c_N = 1.56$, $c_A = 1.01$ (Figure 4). Values of s_n are listed in Table 2.

Errors of the parameters have been estimated from the Monte Carlo simulations using 1000 randomly distributed synthetic data sets (34) of K_n and p parameters. K_n values

Table 3: Partition Functions (Z_n^{apo}) of Helical Segments, Hydrogen Bond Populations (Σw_n) in Apo AcLoopA_nNH₂ Peptides Calculated Using the CAPHELIX Program (35, 36), and Corrections, Arising from Them, to the Free Energies and Enthalpies of La³⁺ Ion Binding

n	Z_n^{apo}	$\delta\Delta G_m$ (cal mol ⁻¹)	Σw_n	$\delta\Delta\Delta H_m$ (cal mol ⁻¹)
0	4.16		0.05	
1	4.48	-40	0.07	-20
2	4.70	-70	0.11	-60
3	5.00	-110	0.18	-130
4	5.30	-150	0.31	-260

have been varied according to normal distribution, with standard deviations determined as described in the Materials and Methods section Fluorescence Measurements. Likewise, the p parameters have been varied with 10% standard deviation (see NMR Measurements in the Materials and Methods) to simulate x_{nNh}^{exp} values.

The errors of c_N and c_A are large: ±0.69 and ±0.46, respectively—because C-cap residue contribution to helix stability is small. The errors of s_n values are given in Table 2.

Corrections Because of Nonrandom Conformation of the Peptides in the Apo State. Because of nonrandom conformation of the apo peptides, ΔG_m values determined from the La³⁺ binding constants are slightly less negative since the free energies of the real conformations are lower than those of random ones. This free energy drop becomes more pronounced with increasing peptide length because of increasing stability of the residual helical conformation. Consequently, s_n parameters shown in Table 2 are smaller than those describing the coil-to-helix transition.

Residual population of the α -helix in metal-free AcLoopA_nNH₂ peptides can be estimated using algorithms and helix propagation parameters available in the literature. Although they have been obtained from studies of much longer helices, our results show that they can be used, as well, in calculation of populations of even very short helical segments (see Discussion).

The program CAPHELIX (35) has been used by us with nucleation and N-cap parameters taken from Chakrabartty et al. (36) and C-cap parameters set equal to 1. Using the van't Hoff relationship with $\Delta H = -900$ cal mol⁻¹ (see ref 37), propagation parameters for 25 °C were calculated from those determined at 1 °C by Chakrabartty et al.

Calculated partition functions Z_n^{apo} , describing the α -helix formation in metal-free AcLoopA_nNH₂ peptides, are listed in Table 3. If -A_nNH₂ segments were in random conformation and did not participate in the helix formation, all Z_n^{apo} values would be the same, equal to Z_0^{apo} . Instead, Z_n^{apo} increases with n because the helix is more stable in longer peptides. A free energy change arising from this effect equals

$$\delta\Delta G_m = -RT \ln(Z_n^{\text{apo}}/Z_0^{\text{apo}}) \quad (16)$$

$\delta\Delta G_m$ values calculated from eq 16 are listed in Table 3, and corrected $\Delta\Delta G_m^* = \Delta\Delta G_m + \delta\Delta G_m$ are given in Table 1.

The helix formation parameters s_n , c_A , and c_N have been recalculated using the corrected free energy values. The populations of full helices x_{nNh}^{cal} remain almost the same (not

Table 4: Enthalpies (in cal mol⁻¹) of La³⁺ Ion Binding to AcLoopA_nNH₂ Peptides (ΔH_m) and Calculated, from Eq 21, the Mean Values of the Helix Propagation Enthalpy (ΔH_{nh})

<i>n</i>	ΔH_m	$\Delta \Delta H_m$	ΔH_{nh}	$\Delta \Delta H_m^a$	ΔH_{nh}^a
0	190				
1	-640	-830	-1140	-850	-1160
2	-960	-1150	-730	-1210	-770
3	-2070	-2260	-980	-2390	-1030
4	-2550	-2740	-990	-3000	-980
mean value			-960		-980

^a Corrected for residual helix content in the metal-free peptides (see text).

shown). Also, the best-fit value (1.56) of c_N does not change. c_A increases from 1 to 1.2. The corrected s_n^* parameters are listed in Table 2.

The mean populations of helical hydrogen bonds per peptide group in -A_nNH₂ segments of the metal-saturated peptides have been calculated from the equations

$$x_{nh} = \left[\frac{c_A}{n+1} \sum_{j=0}^{n-1} (j+1)s_n^j + c_N s_n^n \right] / Z_n \quad (17)$$

for $n \geq 2$ and

$$x_{1h} = (0.5c_A + c_N s_1) / Z_1 \quad (18)$$

for $n = 1$, using the corrected s_n , c_A , and c_N parameters, and the results are listed in the last column of Table 2. They are almost constant, not depending on n , in agreement with the CD data.

Helix Propagation Enthalpy. Analogously to ΔG_m , the total enthalpy of La³⁺ ion binding to AcLoopA_nNH₂ peptides is the sum of enthalpic contributions of conformational rearrangement of the binding loop, ΔH_{Ln} , of the ion coordination, ΔH_{co} , and of the coil-to helix transition within the -A_nNH₂ segment, ΔH_{An} :

$$\Delta H_m = \Delta H_c + \Delta H_{Ln} + \Delta H_{An} \quad (19)$$

Under the assumption that in the apo state the peptide conformation is random

$$\Delta \Delta H_m = \Delta H_{An} - \Delta H_{A0} \quad (20)$$

where ΔH_{An} and ΔH_{A0} denote the enthalpic contributions to free energies ΔG_{An} and ΔG_{A0} , respectively.

Numerous previous studies of helix-coil transition thermodynamics (23, 37–39) have shown that the enthalpy of helix propagation is closely similar for different amino acid residues and may arise predominantly from hydrogen bond formation. Therefore, the contribution of the C-cap alanine and NH₂ groups to the helix formation enthalpy is very close to that of the alanine residues inside the helix. So,

$$\Delta \Delta H_m = [(n+1)x_{nh} - x_{0h}] \Delta H_{nh} \quad (21)$$

where ΔH_{nh} denotes a mean value of the helix propagation enthalpy in AcLoopA_nNH₂ peptides.

ΔH_m values determined from calorimetric measurements are listed in Table 4. Within error, they change linearly with a slope of -690 cal mol⁻¹ per alanine residue (see Figure 5). Such dependence is expected from eq 21, if ΔH_{nh} is constant, since x_{nh} is almost the same (~ 0.72) for $n \geq 1$

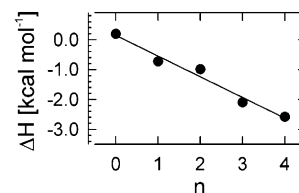


FIGURE 5: Heat effect, determined by calorimetric measurements, of La³⁺-ion binding to AcLoopA_nNH₂ peptides.

(see Table 2). Consequently, the average helix propagation enthalpy can be estimated to be $\Delta H_h = -690/0.72 = -960$ cal mol⁻¹. The average of all ΔH_{nh} values calculated with eq 21 is exactly the same (see Table 4).

Similarly as free energies, $\Delta \Delta H_m$ should be corrected for the residual helicity of the apo peptides. The populations of helical hydrogen bonds in the metal-free AcLoopA_nNH₂ peptides ($\sum w_n$) have been calculated using the CAPHELIX program (35, 36) and are listed in Table 3. The corrections that should be added to the experimental $\Delta \Delta H_m$ values equal:

$$\delta \Delta \Delta H_m^* = (\sum w_n - \sum w_0) \Delta H_{nh} \quad (22)$$

They have been calculated for $\Delta H_{nh} = 1$ kcal mol⁻¹ (see Table 3). The corrected $\Delta \Delta H_m^*$ and corresponding ΔH_{nh}^* values are listed in Table 4. The corrected average ΔH_h value equals -980 cal mol⁻¹.

DISCUSSION

Helix Propagation Parameters. It should be noted that formally the s_n parameters measured by us do not correspond exactly to those defined by the Zimm–Bragg theory because they are not the coil to α -helix but rather the coil to helix transition parameters. That is, they describe the process of restriction of polypeptide backbone torsional angles to the helical region of the Ramachandran plot, without specifying whether i to $i+4$ or i to $i+3$ bonds between CO and NH main chain groups are formed. NMR conformational studies of AcLoopA_nNH₂ peptides (unpublished results) indicate that the 3_{10} helix conformation predominates in AcLoopANH₂ and AcLoopA₂NH₂ peptides and that the regular α -helical conformation is assumed by one, then by two alanine residues immediately following the metal-binding loop in longer peptides: AcLoopA₃NH₂ and AcLoopA₄NH₂, respectively. These findings confirm earlier results of NMR conformational studies of Ala-rich peptides (14).

Moreover, molecular dynamics studies of helix propagation indicate (11) that the propagation parameters s_n can be different at N- and C-termini of a helix. The s_n values determined by us describe, of course, the helix propagation at the C-terminus, which is supposed to be less favorable than at the N-terminus.

The error of the s_1 parameter is very large (± 0.60) because the contribution of free energy of one alanine residue to a 70% populated helix is small and cannot be measured precisely. The error of s_2 is smaller but still considerable (± 0.21). In fact, the first four steps of the helix propagation in polyalanine can be described by weighted average parameter $s = 1.54 \pm 0.04$. It is close to, but noticeably higher than, $s_\infty = 1.3$ —the propagation parameter in long polyalanine-based peptides, determined by Chakrabarty et al. (36) at 1 °C and extrapolated to 25 °C according to the van't Hoff relationship with $\Delta H = 1$ kcal mol⁻¹. Therefore,

our conclusion is that various effects that may both increase and decrease the initial helix propagation parameters cancel each other, to a large extent, at least in the case of polyaniline, and that the stability of very short helices is described by propagation parameters only slightly greater than those determined from studies of long polypeptide chains.

From studies of polyaniline peptides linked at N-terminus to a synthetic helix-inducing template (40), Kemp et al. deduced that the helix propagation constant for alanine is close to 1 and that a high helix content in the alanine-based peptides used by Baldwin and co-workers (36) must be explained rather by high helix-stabilizing propensities of some other residues (e.g., lysine (41)) than these peptides also contain. The same view was expressed recently by Scheraga (42).

We have studied the helix propagation in peptide segments built only of alanine. Our results show that alanine is a strong helix-maker in short helices. Since s_3 and s_4 , determined by us with high precision, are nearly the same (1.59 ± 0.08 and 1.50 ± 0.05 , respectively) some drop of s with the helix length is possible but certainly not so dramatic as to reach a value close to 1 for s_∞ . Therefore, our results strongly support the arguments presented by Rohl et al. (43) in their discussion with Kemp and co-workers (40, 41).

On the other hand, some of our data seem to indicate that glutamine—one of amino acid residues present in Baldwin's model peptides—can play some special role in helix stabilization. In our previous study (24), we have found that the helix content in -AlaAlaAlaGlnNH₂ segment (-A₃QNH₂ using our present notation) attached to the La³⁺ saturated AcLoop- exceeds 0.8. Lopez et al. (37) estimated its value to be greater than 0.95. Interestingly, the helix content of the -A₄NH₂ segment of the La³⁺ saturated AcLoopA₄NH₂ peptide is considerably lower (0.74, see Table 2). This finding is directly confirmed by a relatively low CD signal at 222 nm in the AcLoopA₄NH₂—AcLoopNH₂ difference spectrum (2350 deg cm² dmol⁻¹, see Figure 2b) when compared with that of AcLoopA₃QNH₂—AcLoopNH₂ (3250 deg cm² dmol⁻¹, see ref 24). Such a high helix content in the AcLoopA₃QNH₂ peptide was explained by us (24) by assuming very high values of the helix propagation parameters in short polyaniline segments. In light of the present results, this explanation appears to be false. Therefore, the only possible conclusion seems to be that the Gln-NH₂ group provides an extremely effective C-cap box stabilizing the helical conformation. If the alanine propagation parameters are practically the same, independent of n , its C-cap parameter should also be constant, as we had initially assumed when formulating eqs 6 and 7.

The C-cap parameters of all 20 amino acid residues and the NH₂ group have been published by Doig and Baldwin (44); however, these are all relative C-cap values. With the system that we have used, determination of the absolute values of c_N and c_A has been possible although within large error limits. Their ratio (1.3) is exactly the same as that determined by Doig and Baldwin. We propose that the C-cap parameters, published by these authors, can be transferred from relative into absolute ones, by attributing to alanine a C-cap value of 1.2.

Helix Propagation Enthalpy. The precision of our calorimetric measurements (see Materials and Methods) allows us to determine $\Delta\Delta H_m$ within an error of ~ 200 cal mol⁻¹

for $n = 1$ down to ~ 100 cal mol⁻¹ for $n = 4$. Within these limits, the enthalpy of the first four steps of the helix propagation in polyaniline remains constant and its average value $\Delta H_h = -980 \pm 100$ cal mol⁻¹.

Recently (37), the helix propagation enthalpy in polyaniline has been determined by Lopez et al. from comparative calorimetric measurements of the heat of La³⁺ ion binding to AcLoopNH₂, AcLoopA₃QNH₂, and AcLoopA₆QNH₂ peptides (according to the notation used in this paper). These authors found ΔH_h for both -A₃QNH₂ and -A₆QNH₂ segments to be the same, equal to -0.9 ± 0.1 kcal mol⁻¹.

We believe that this value is slightly too low because of the overestimation of the helix content in the La³⁺ saturated peptides. CD measurements made by Lopez et al. have shown that it equals at least 95%. That seems to be also the upper limit of the helix population because its higher value can be explained only by an excessively strong helix stabilizing effect of the C-terminal QNH₂ group. Nevertheless, the calorimetric data are treated by Lopez et al. as corresponding to a transition from roughly 50% helix population in the apo states of the peptides (see Figure 5 in ref 37) to 100% in their met form. If this last value equals, in fact, 95%, the ΔH_h found by Lopez et al. must be corrected by 10% and then becomes the same as that found by us. Previously, the enthalpy of helix propagation in polyaniline was estimated at roughly -1 kcal mol⁻¹ from calorimetric measurements of the heat effects of thermal unfolding of a 50-residue, alanine-based peptide (38). Also, values of ΔH_h in the neighborhood of -1 kcal mol⁻¹ have been found from calorimetric studies of different model peptides: poly-L-glutamate (45) (-1.1 ± 0.2 kcal mol⁻¹), poly-L-lysine (46) (-1.3 ± 0.1 kcal mol⁻¹), AcY(MEARA)₆-NH₂ peptide (39) (-840 cal mol⁻¹, given without estimation of error limits), and a dicyclic 29-residue peptide (23) KDAAARARKET-NRRAAARSQKRAAKRDA (-650 ± 50 cal mol⁻¹); earlier estimates of -1.1 kcal mol⁻¹ for poly-L-glutamate and -0.89 kcal mol⁻¹ for poly-L-lysine (47) had been based on measured temperature dependence of s .

ACKNOWLEDGMENT

We thank Jan Hermans for his help in thermodynamic analysis of the experimental data and correction of the text, Andrzej Ejchart for NMR data discussion and his help in error calculations, and Michal Dadlez for his critical review of the manuscript.

REFERENCES

1. Rohl, C. A., and Baldwin, R. L. (1998) *Methods Enzymol.* 295, 1–26.
2. Kallenbach, N. R., and Spek, E. J. (1998) *Methods Enzymol.* 295, 26–41.
3. Munoz, V., and Serrano, L. (1994) *Nature Struct. Biol.* 1, 399–409.
4. Zimm, B. H., and Bragg, J. K. (1959) *J. Chem. Phys.* 31, 526–535.
5. Lifson, S., and Roig, A. (1961) *J. Chem. Phys.* 34, 1963–1974.
6. Chakrabarty, A., and Baldwin, R. L. (1995) *Adv. Protein Chem.* 46, 141–176.
7. Doig, A. (2002) *Biophys. Chem.* 101–102, 281–293.
8. Bierzynski, A., and Pawlowski, K. (1997) *Acta Biochim. Pol.* 44, 423–432.
9. Avbelj, F., Luo, P., and Baldwin, R. L. (2000) *Proc. Natl. Acad. Sci. U.S.A.* 97, 10786–10791.

10. Aqvist, J., Luecke, H., Quijcho, F. A., and Warshel, A. (1991) *Proc. Natl. Acad. Sci. U.S.A.* 88, 2026–2030.
11. Young, W. S., and Brooks, C. L., III (1996) *J. Mol. Biol.* 259, 560–572.
12. Sheinerman, F. B., and Brooks, C. L., III (1995) *J. Am. Chem. Soc.* 117, 10098–10103.
13. Rohl, C. A., and Doig, A. J. (1996) *Protein Sci.* 5, 1687–1696.
14. Millhauser, G. L., Stenland, C. J., Hanson, P., Bolin, K. A., and van de Ven, F. J. M. (1997) *J. Mol. Biol.* 267, 963–974.
15. Barlow, D. J., and Thornton, J. M. (1988) *J. Mol. Biol.* 201, 601–619.
16. Ruan, F., Chen, Y., and Hopkins, P. B. (1990) *J. Am. Chem. Soc.* 112, 9403–9404.
17. Jackson, D. Y., King, D. S., Chmielewski, J., Singh, S., and Schultz, P. G. (1991) *J. Am. Chem. Soc.* 113, 9391–9392.
18. Kemp, D. S., Boyd, J. G., and Muendel, C. C. (1991) *Nature* 352, 451–454.
19. Osapay, G., and Taylor, J. W. (1992) *J. Am. Chem. Soc.* 114, 6966–6973.
20. Zhou, H. X., Hull, L. A., and Kallenbach, N. R. (1994) *J. Am. Chem. Soc.* 116, 6482–6483.
21. Luo, P., Braddock, D. T., Subramanian, R. M., Meredith, S. C., and Lynn, D. G. (1994) *Biochemistry* 33, 12367–12377.
22. Phelan, J. C., Skilton, N. J., Braisted, A. C., and McDowell, R. S. (1997) *J. Am. Chem. Soc.* 119, 455–460.
23. Taylor, J. W., Greenfield, N. J., Wu, B., and Privalov, P. L. (1999) *J. Mol. Biol.* 291, 965–976.
24. Siedlecka, M., Goch, G., Ejchart, A., Sticht, H., and Bierzynski, A. (1999) *Proc. Natl. Acad. Sci. U.S.A.* 96, 903–908.
25. *Handbook of Biochemistry and Molecular Biology* (1976) (Fasman, G. D., Ed.) 3rd ed., Vol. 1, CRC Press, Cleveland.
26. Dadlez, M., Goral, J., and Bierzynski, A. (1991) *FEBS Lett.* 282, 143–146.
27. Forsen, S., and Hoffman, R. A. (1963) *J. Chem. Phys.* 39, 2892–2901.
28. Piotto, M., Saudek, V., and Sklenar, V. (1992) *J. Biomol. NMR* 2, 661–665.
29. Vold, R. L., Waugh, J. S., Klein, M. P., and Phelps, D. E. (1968) *J. Chem. Phys.* 48, 3831–3832.
30. Wiseman, T., Williston, S., Brandts, J. F., and Lin, L. N. (1989) *Anal. Biochem.* 179, 131–137.
31. Nelder, J. A., and Mead, R. (1965) *Computer J.* 7, 308–313.
32. Woody, R. W., and Koslowski, A. (2002) *Biophys. Chem.* 101–102, 525–551.
33. Chen, Y.-H., Yang J. T., and Chau, K. H. (1974) *Biochemistry* 13, 3350–3359.
34. Press, W. H., Flannery, B. P., Teukolsky, S. A., and Vetterling, W. T. (1986) *Numerical Recipes*, Cambridge, Cambridge University Press, p 818.
35. Doig, A. J., Chakrabarty, A., Klingler, T. M., and Baldwin, R. L. (1994) *Biochemistry* 33, 3396–3403.
36. Chakrabarty, A., Kortemme, T., and Baldwin, R. L. (1994) *Protein Sci.* 3, 843–852.
37. Lopez, M. M., Chin, D.-H., Baldwin, R., and Makhatadze, G. I. (2002) *Proc. Natl. Acad. Sci. U.S.A.* 99, 1298–1302.
38. Scholtz, J. M., Marqusee, S., Baldwin, R. L., York, E. J., Stewart, J. M., Santoro, M., and Bolen, D. W. (1991) *Proc. Natl. Acad. Sci. U.S.A.* 88, 2854–2858.
39. Richardson, J. M., McMahon, K. W., MacDonald, C. C., and Makhatadze, G. I. (1999) *Biochemistry* 38, 12869–12875.
40. Kemp, D. S., Oslick, S. L., and Allen, T. J. (1996) *J. Am. Chem. Soc.* 118, 4249–4255.
41. Williams, L., Kather, K., and Kemp, D. S. (1998) *J. Am. Chem. Soc.* 120, 11033–11043.
42. Scheraga, H. A., Vila, J. A., and Ripoll, D. R. (2002) *Biophys. Chem.* 101–102, 255–265.
43. Rohl, C. A., Fiori, W., and Baldwin, R. L. (1999) *Proc. Natl. Acad. Sci. U.S.A.* 96, 3682–3687.
44. Doig, A. J., and Baldwin, R. L. (1995) *Protein Sci.* 4, 1325–1336.
45. Rialdi, G., and Hermans, J., Jr. (1966) *J. Am. Chem. Soc.* 88, 5719–5720.
46. Chou, P. Y., and Scheraga, H. A. (1971) *Biopolymers* 10, 657–680.
47. Hermans, J. (1966) *J. Phys. Chem.* 70, 510–515.

BI027339D